Journal of Solid State Chemistry **154,** 87–92 (2000)
doi:10.1006/jssc.2000.8816, available online at http://www.idealibrary.com on IDEAL®

# Interband Transitions, IR-Active Phonons, and Plasma Vibrations of Some Metal Hexaborides

H. Werheit, T. Au, and R. Schmechel[1]

*Solid State Physics Laboratory, Gerhard-Mercator University of Duisburg, D-47048 Duisburg, Germany*

and

Yu. B. Paderno and E. S. Konovalova

*I.N. Frantsevich Institute for Problems of Materials Science, Ukrainian Academy of Sciences, 252142 Kiev Ukraine*

Received September 9, 1999; in revised from January 24, 2000; accepted January 30, 2000

**The high IR reflectivity of monocrystalline metallic metal hexaborides is superimposed by weak phonon spectra. The symmetry selection rules are lifted, probably because of structural defects. From the plasmon–phonon polariton frequencies in metallic $LaB_6$ compared with those in semiconducting $EuB_6$ and $YbB_6$, the softening and the hardening of specific $F_{1u}$ modes by the free carriers are determined. From the plasma edges of $EuB_6$ and $YbB_6$, some parameters of the electronic transport are derived. The electron concentration increases proportional to the C content, whose donor properties are found to be comparable to those of hydrogen-like impurities. The existence of energy gaps in $EuB_6$ and $YbB_6$ proves that these compounds are semiconductors.** 

## INTRODUCTION

The unit cell of the cubic structure contains one formula weight of $MB_6$. Most of the rare-earth metals and moreover Ca, Sr, Ba, Th, Np, Pu, and Am form isostructural hexaborides. The boron atoms are arranged in regular octahedra positioned at the corners of the unit cell, whose center is occupied by the metal atom. The metal hexaborides are interesting materials for fundamental science and application as well. For application their low work functions combined with high melting points are important. In fundamental science at present the influence of structural defects on the various physical properties is in the foreground of interest, and in some cases the question is whether the compounds are semiconductors or semimetals. The IR optical investigations in the present paper were performed to contribute to the solution of these questions.

## SAMPLE MATERIAL

Pure single-crystal metal hexaborides $YB_6$, $LaB_6$, $CeB_6$, $SmB_6$, $Sm_{0.8}B_6$, and $TbB_6$ (metal-like) and $EuB_6$ and $YbB_6$ (semiconducting) were investigated. The source borides were obtained by the reduction of high-purity metal oxides with amorphous boron in vacuum. The crystals were grown by the induction zone melting method under argon at pressures between 1.5 and 18 atm, depending on the specific compound. The purity is typically better than 99.5%; usually there are certain deficiencies in both sublattices. The C content is not higher than 0.1% (however see Fig. 7). Additionally, sintered polycrystalline $EuB_6$ (ESK) with a C content of 1.1 at.% and sintered $EuB_{6-X}C_X$ ($X \sim 0.1$) (ESK) (C = 1.43 at.%) (1) are investigated.

## RESULTS

### *(a) Semiconducting Metal Hexaborides*

The reflectivity spectra of the semiconducting $EuB_6$ and $YbB_6$ are presented in Fig. 1. For the pure single crystals the spectra are obviously essentially determined by the plasma edges of free carriers. In agreement with group theory two phonons are clearly seen. However, the dispersion curves in the range of these resonances suggest that they are to be attributed to plasmon–phonon polaritons, whose frequency is shifted by the plasmon–phonon interaction (2, 3).

For metallic $LaB_6$ and $SmB_6$ the phonon frequencies 214 $cm^{-1}$ (in good agreement with our result in Table 1) and 172 $cm^{-1}$, respectively, were obtained by Raman spectroscopy in (5). The comparison with our data for the

[1]Present address: Darmstadt University of Technology, Material Science, Department of Electronic Materials, D-64287 Darmstadt, Germany.



0022-4596/00 $35.00

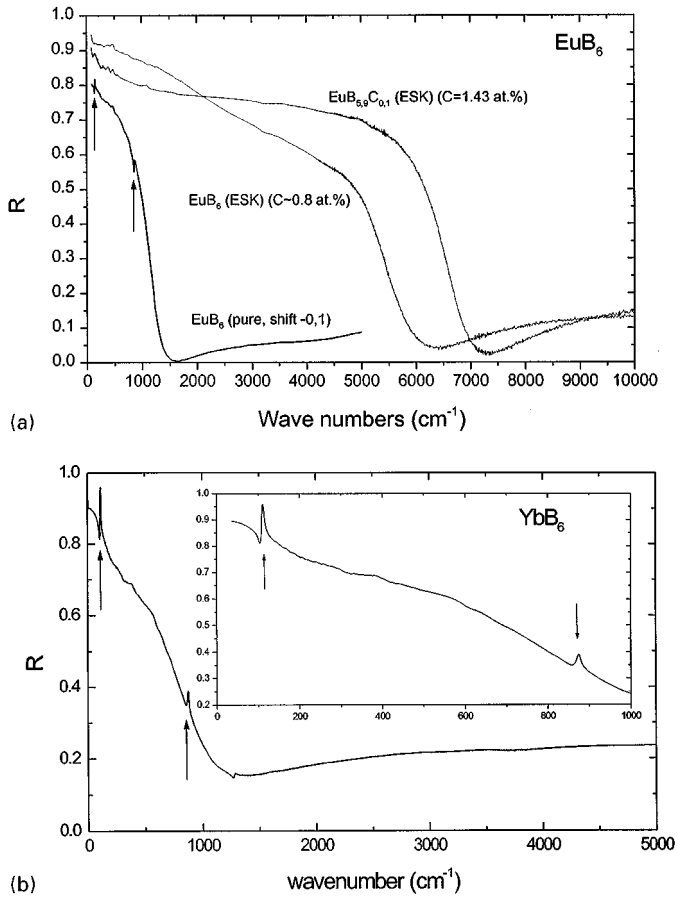


**FIG. 1.** IR reflectivity spectrum of (a) single-crystal pure and polycrystalline carbon-doped $EuB_6$ and (b) single-crystal pure $YbB_6$. The plasmon–phonon polaritons are indicated by arrows.

semiconducting $EuB_6$ and $YbB_6$ clearly shows the influence of the carrier concentration on the phonon frequencies.

The absorption spectra of $EuB_6$ and $YbB_6$ determined from the reflectivity spectra by a Kramer–Kronig transformation are displayed in Fig. 2. At low frequencies, the absorption decreasing with decreasing energy indicates that the free carrier absorption has no significant influence in this range. Therefore, assuming phonon scattering, an empirical slope for the maximum free carrier absorption is calculated, which is fitted to the lowest absorption at the low-energy end of the measured spectra.

**TABLE 1**
**Plasmon–Phonon Polariton Frequencies of $F_{1u}$ Phonon Modes in Semiconducting and Metallic Metal Hexaborides**

| Compound | $\nu_1(\mathrm{cm}^{-1})$ | $\nu_2(\mathrm{cm}^{-1})$ |
|---|---|---|
| Semiconductors | | |
| $EuB_6$ | 146 | 858.5 |
| $YbB_6$ | 109 | 868 |
| Metal | | |
| $LaB_6$ | 207.3 | 498.4 |

### *(b) Metallic Metal Hexaborides*

For the metallic hexaborides the plasma edges are far outside the investigated spectral range. Accordingly, in the range below 5000 $\mathrm{cm}^{-1}$ only the high reflectivity due to the negative real part of the dielectric function is seen in Fig. 3. In the phonon range ($<1500\ \mathrm{cm}^{-1}$) the high reflectivity is superimposed by a weak structure, which is similar for the different compounds, only slightly shifted in frequency for the individual hexaborides. The only exception is $LaB_6$, showing only two but more significant dispersive structures in the spectral range of phonons (Fig. 4). Surprisingly, the phonon spectrum of $Sm_{0.8}B_6$ is much weaker than that of $SmB_6$, in contrast to a higher defect concentration in $Sm_{0.8}B_6$ expected because of the considerable metal deficiency.

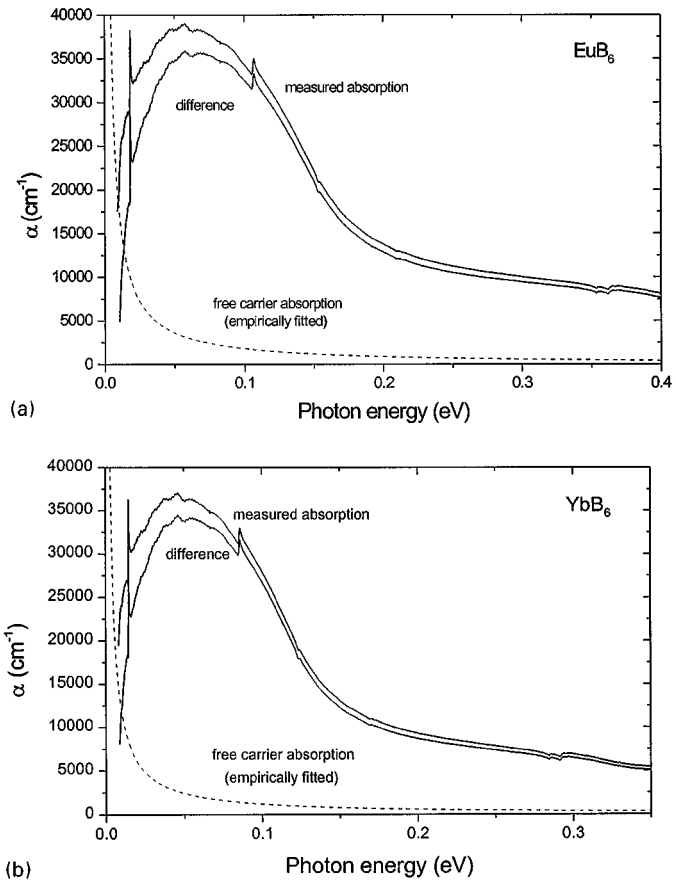


**FIG. 2.** IR absorption spectrum of (a) $EuB_6$ and (b) $YbB_6$ calculated from the reflectivity spectra in Fig. 1 using a Kramers–Kronig transformation. An empirical slope for the free carrier absorption ($\propto \lambda^2$ for phonon scattering) is calculated.

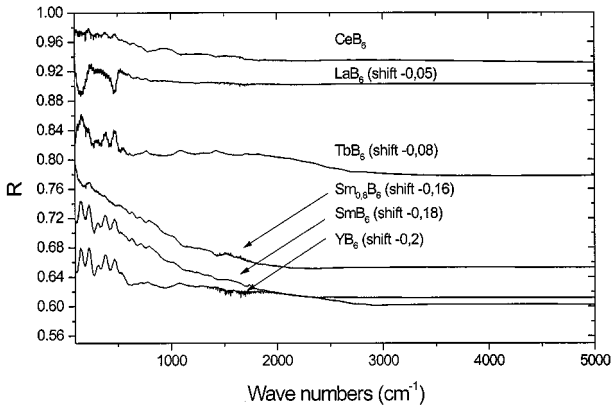


**FIG. 3.** IR reflectivity spectra of single-crystal pure $YB_6$, $LaB_6$, $CeB_6$, $SmB_6$, $Sm_{0.8}B_6$, and $TbB_6$. Some of the spectra are vertically shifted to avoid superposition. The amount of the shifts are indicated next to the spectra.

## DISCUSSION

### (*a*) *Phonons*

The optical vibration modes of the $MB_6$ compounds at the $\Gamma$ point are described (4) by

$$\Gamma_{opt} = A_{1g} + E_g + F_{1g} + F_{2g} + 2F_{1u} + F_{2u},$$

where an additional $F_{1u}$ mode is acoustical. The $A_{1g}$, $E_g$, and $F_{2g}$ modes are Raman active and the two $F_{1u}$ modes are IR active. However, it is well known that even high-purity carefully prepared single crystals of the metal hexaborides exhibit considerable structural defects, in particular vacancies in the boron and metal sublattices. With these defects the lifting of the symmetry selection rules in the Raman spectra was qualitatively explained (5–7). Therefore it is expected that the IR phonon spectra as well are not restricted to the IR-active phonons, and this suggests to interpret the weak structures in the reflectivity spectra accordingly. Apart from the structural defects mentioned, there are structural distortions in boron compounds with natural isotope enrichment ($\sim$19% $^{10}$B, $\sim$81% $^{11}$B) because the isotopes have remarkably different zero-point energies. Numerous investigations on the phonon spectra in icosahedral boron-rich solids suggest that these distortions are not sufficient to lift the symmetry selection rules; a final decision, however, is still open. In Fig. 5 the phonon frequencies of the metallic hexaborides found in the IR spectra follow the same tendencies as those obtained by Raman spectroscopy (8) For $SmB_6$ it is shown in Fig. 6 that the maxima of the phonon absorption bands well agree with the phonon DOS maxima determined by neutron scattering (9), irrespective of the symmetry selection rules. In the FT Raman spectrum (7) included in Fig. 6 for comparison, the peak correlated with the lowest frequency optical vibration at the $\Gamma$ point is considerably shifted toward frequencies lower than that of the IR absorption spectrum. Taking into

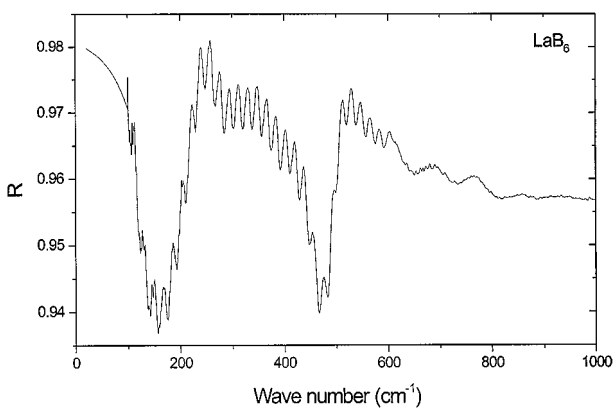


**FIG. 4.** IR reflectivity of $LaB_6$ in the spectral range of the plasmon–phonon polaritons. The interferences are probably not an effect from the sample.

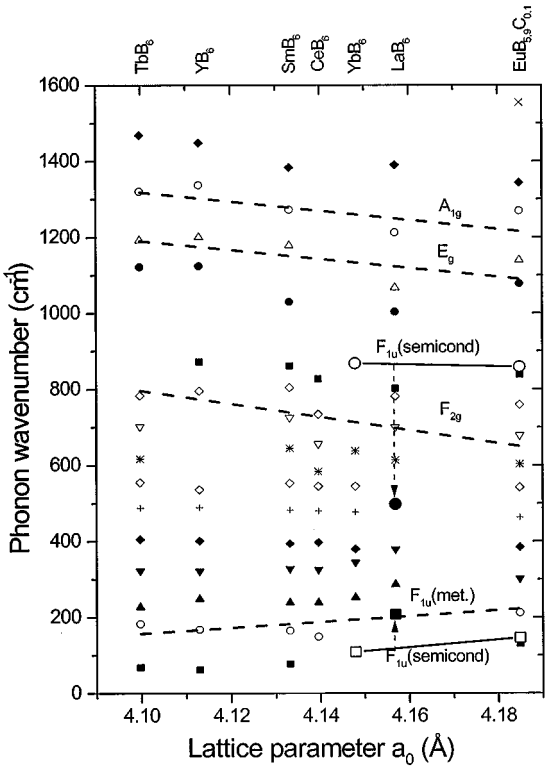


**FIG. 5.** Phonon frequencies obtained from the IR absorption spectra (calculated from the measured reflectivity spectra by the Kramers–Kronig transformation). The same symbols are used for phonons in different compounds, which can probably be attributed to one another. The dashed lines represent the Raman frequencies measured in (8). The solid lines combine the polaritons of the semiconducting hexaborides $EuB_6$ and $YbB_6$, and the arrows indicate the shift to the related resonance frequency in $LaB_6$ (see Table 1).

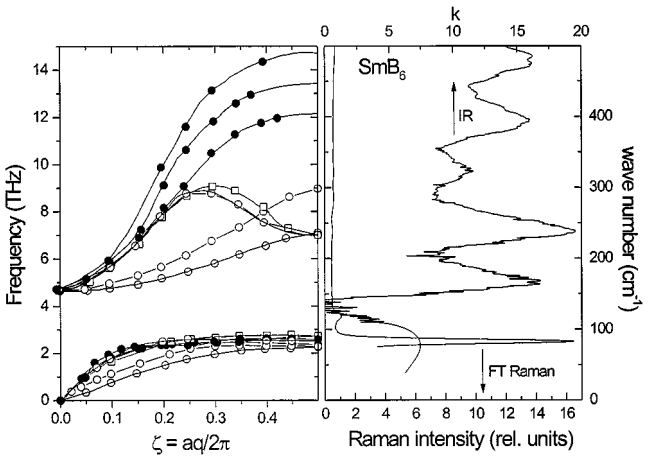


**FIG. 6.** Phonon absorption spectrum of $SmB_6$ ($k$, absorption index) compared with the FT Raman spectrum (7) measured on the same sample and phonon dispersion curves (collected for all crystallographic directions) reproduced from (9).

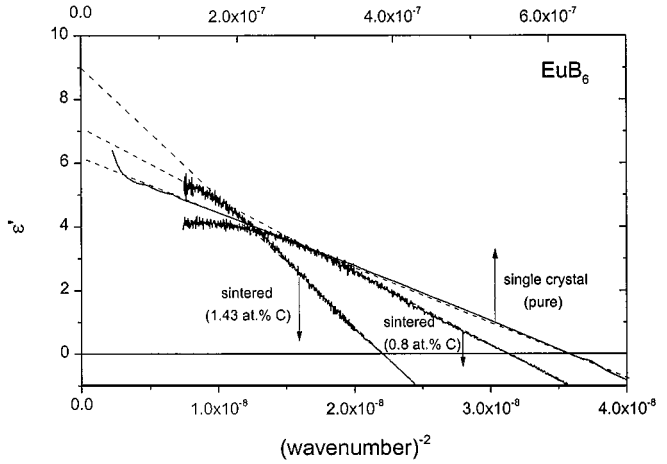


**FIG. 7.** Real part of the dielectric function of $EuB_6$ vs the squared reciprocal wavenumber.

account that both results were obtained on the same sample, one comes to the conclusion that the high 4-W excitation power of the Nd:YAG laser in the FT Raman spectrometer causes the softening of this phonon mode from 157 $cm^{-1}$ (IR, this paper) to 118 $cm^{-1}$ (FT Raman) (7) (small peak of the Raman spectrum in Fig. 6). The obvious reason is that the density of carriers in the intermediate valent $SmB_6$ is considerably changed by the optical excitation, while it remains largely unchanged in metallic $LaB_6$ (7).

The shift of the polariton frequencies from the semiconducting $EuB_6$ and $YbB_6$ to the metallic $LaB_6$ makes it possible to quantitatively estimate the softening of the high-frequency $F_{1u}$ mode by $-362\ cm^{-1}$ and the hardening of the low-frequency $F_{1u}$ mode by $+91.6\ cm^{-1}$ (see indication by arrows in Fig. 5). This shift is obviously due to the higher carrier concentration in metallic $LaB_6$, which after Grushko *et al.* (10) exceeds that in semiconducting $EuB_6$ and $YbB_6$ by about two orders of magnitude.

### (*b*) *Plasma Vibrations*

The plasma edges in the reflectivity spectra of $EuB_6$ and $YbB_6$ can be well described by the classical Drude theory. For $\omega_\tau \ll \omega_p$ the expected linear slope of $\varepsilon'$ vs $1/\omega^2$ according to $\varepsilon' = \varepsilon_L - (\omega_p^2/\omega^2)$ yields the dielectric constant of the lattice $\varepsilon_L$ by extrapolation to $1/\omega^2 = 0$ and the plasma resonance frequency $\omega_p$ by extrapolation to $\varepsilon' = 0$ (for $EuB_6$ see Fig. 7). The results are listed in Table 2. Using the average effective mass of free carriers determined for $EuB_6$ from magnetoresistance experiments (11), the carrier concentrations of our $EuB_6$ samples were determined.

In Fig. 8 (results partly obtained from (12)), it is shown that the carrier concentration of $EuB_6$ is largely proportional to the carbon content. Schwetz *et al.* (14) proved that the lattice parameter of $EuB_{6-x}C_x$ decreases linearly with the carbon content up to the solution limit. This excludes the interstitial accommodation of carbon atoms that would cause a dilatation of the structure. Therefore we assume that the carrier concentration comes essentially from a donor level generated by C atoms substituting for regular B atoms. The ionization energy of this donor level can be roughly estimated: With the lattice parameter $a = 4.185$ Å one obtains for 1 at.% carbon $9.55 \times 10^{20}$ C atoms $cm^{-3}$, which—according to Fig. 8—provide $4.8 \times 10^{20}$ electrons $cm^{-3}$ at 300 K. Then

$$\delta E(\text{C in } EuB_6) = k_B T \ln (N_C/n_e) \sim 18\ \text{meV}.$$

**TABLE 2**
**Some Electronic Transport Parameters of Semiconducting Metal Hexaborides at 300 K**

| Compound | $\varepsilon_L$ | $\omega_p$ ($s^{-1}$) | $m_n^*/m_0$ | Direction of calculation | $n_e$ ($cm^{-3}$) |
|---|---|---|---|---|---|
| $EuB_6$ (single crystal) | 6.1 (1) | $2.4 \times 10^{14}$ | 0.225 (11) | → | $2.5 \times 10^{19}$ |
| $EuB_6$ (ESK, sintered) | 7.0 (1) | $9.1 \times 10^{14}$ | 0.225 (11) | → | $4.1 \times 10^{20}$ |
| $EuB_{5.9}C_{0.1}$ (ESK, sintered) | 8.9 (1) | $1.1 \times 10^{15}$ | 0.225 (11) | → | $7.8 \times 10^{20}$ |
| $YbB_6$ (single crystal) | 7.0 (2) | $1.7 \times 10^{14}$ | 0.47 | ← | $3.1 \times 10^{19}$ |

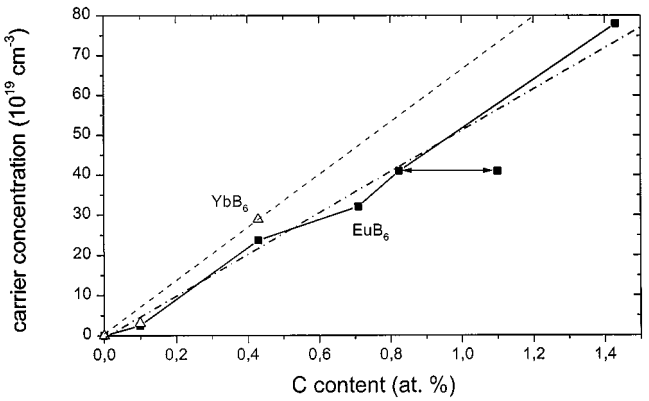


**FIG. 8.** Carrier concentration vs C content; data at C = 0.43 and 0.71 at.% from (12). The points for the pure crystals investigated in the present paper suggest that the upper limit of 0.1 at.% is too high and the real C content is only about 0.05 at.%. The arrow marks the relation between the chemically determined total C content of 1.1 at.% and that in the $EuB_6$ lattice, which according to experience is roughly estimated to be about 25% lower in sintered $EuB_6$ (13).

Unfortunately in the case of $YbB_6$ the relation between carrier and carbon concentration is available for only one compound (12). If one assumes the same dependence as in $EuB_6$ between electron concentration and carbon content one obtains

$$\delta E(\text{C in } YbB_6) \sim 11 \text{ meV}.$$

These values are compatible with the ionization energies of hydrogen-like impurities in classical semiconductors and satisfactorily agree with transition no. 2 of both compounds in Table 3 determined from the decomposition of the absorption edge (see below).

Because of the same preparation method we assume that the C contents of our $EuB_6$ and $YbB_6$ crystals are nearly the same. Therefore, from the relation $n(YbB_{5.97}C_{0.03})/n(EuB_{5.97}C_{0.03}) = 1.22$ (12), we estimated for our $YbB_6$ sample the carrier concentration and from that the effective mass in Table 2.

**TABLE 3**
**Optical Transition Energies $\Delta E$ of the Semiconducting $EuB_6$ and $YbB_6$**

| No. | $EuB_6$ $\Delta E$ (meV) | $EuB_6$ (ESK) $\Delta E$ (meV) | $YbB_6$ $\Delta E$ (meV) | Type of Transition |
|---|---|---|---|---|
| 1 | 9.55(10) | 7.6(3) | 7.45(5) | Impurity to band |
| 2 | 13.2(3) | 15 (1) | 10.4(2) | Impurity to band or direct–forbidden interband |
| 3 | 20.1(5) | — | 15.2(5) | Direct-allowed interband |
| 4 | 32.8(2) | 34 (3) | 26.0(4) | Direct-allowed interband |

(*c*) *Interband Absorption*

The strength of the absorption in Figs. 2a and 2b respectively ($\alpha > 10^4$ cm$^{-1}$) indicates electronic interband transitions. The absorption edges of $EuB_6$ and $YbB_6$ are shown in a higher resolution in Figs. 9a and 9b. The distinct peaks at 18.2 and 14.6 meV were attributed to polaritons (see above) because electronic transitions at this energy should be largely smoothed at 300 K.

The absorption edge was decomposed step by step into several electronic transitions using a local computer program, which makes it possible to fit the different theories of interband transitions (see, e.g., (15)) or impurity level absorption (16) to the measured spectra and easy to decide which fit is the best.

The existence of energy gaps of $EuB_6$ and $YbB_6$ definitely proves that these metal hexaborides are semiconductors and not semimetals, contrary to the conclusion (for $EuB_6$) by Aronson *et al.* (11) and to the band structure calculation by Hasegawa and Yanase (17).

In agreement with numerous investigations of other authors on metal hexaborides, in the present paper it became evident that structural defects play an important role in these solids, even if the crystals are very carefully prepared. For icosahedral boron-rich solids containing

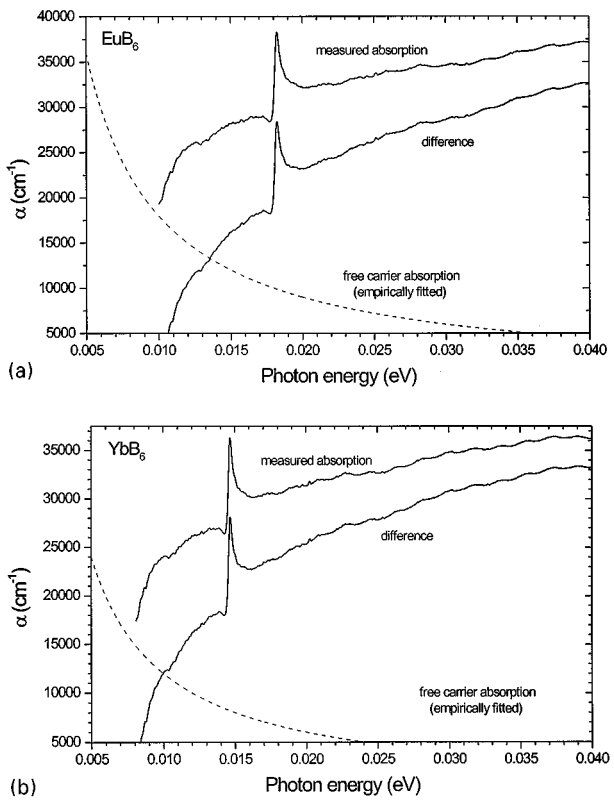


**FIG. 9.** Absorption edge of (a) $EuB_6$ and (b) $YbB_6$. For free carrier absorption see the text in connection with Fig. 2.

considerable defect concentrations as well, it has recently been proved that the structural defects are immediately correlated with the electronic properties in a way that defects are generated to transform the crystal into an apparently energetically more favorable state of a semiconductor, compared with the theoretical band structure calculations on hypothetical undistorted structures indicating metallic behavior (18, 19). This could hold in the case for the metal hexaborides as well, and could, for example be, the reason that in $Sm_{0.8}B_6$ the lattice distortions are considerably lower than those in $SmB_6$ (see above).

## ACKNOWLEDGMENT

The authors are grateful to Dr. K. A. Schwetz, Elektroschmelzwerk Kempten, for providing the carbon-doped $EuB_6$ samples and their chemical analysis.

## REFERENCES

1. H. Knoch, K. A. Schwetz, E. Bechler, and A. Lipp, *in* "Proceedings 9th International Symposium Boron, Borides and Related Compounds, University of Duisburg, Duisburg, Germany, Sept. 21–25, 1987" (H. Werheit, Ed.), p. 442.
2. E. Gerlach and P. Grosse, *in* "Advances in Solid State Physics" (J. Treusch, Ed.), Vol. 17, p. 157. Vieweg, Braunschweig, 1977.
3. P. Grosse, "Freie Elektronen in Festkörpern," Springer-Verlag, Berlin, 1979.
4. Z. Yahia, S. Turrell, J.-P. Mercurio, and G. Turrell, *J. Raman Spectrosc.* **34,** 307 (1993).
5. I. Mörke, V. Dvorak, and P. Wachter, *Solid State Commun.* **40,** 331 (1981).
6. G. Schell, H. Winter, H. Rietschel, and F. Gompf, *Phys. Rev. B* **25,** 1589 (1982).
7. R. Schmechel, H. Werheit, and Y. Paderno, *J. Solid State Chem.* **133,** 264 (1997).
8. E. Zirngiebl, S. Blumenröder, R. Mock, and G. Güntherodt, *J. Magn. Magn. Matero* **54–57,** 359 (1986).
9. P. A. Alekseev, A. S. Ivanov, K. A. Kikoin, A. S. Mischenko, A. N. Lasukov, A. Yu. Rumyantsev, I. P. Sadikov, E. S. Konovalova, Yu. B. Paderno, B. Dorner, and H. Shober, *in* "Boron-Rich Solids, Proceedings 10th International Symposium on Boron, Borides, and Related Compounds, Albuquerque, NM, 1990" (D. Emin, T. L. Aselage, A. C. Switendick, B. Morosin, and C. L. Beckel, Eds.), AIP Conf. Proc. 231, p. 318. American Institute of Physics, New York, 1991.
10. Yu. S. Grushko, Yu. B. Paderno, K. Ya. Mishin, L. I. Molkanov, G. A. Shadrina, E. S. Konovalova, and E. M. Dudnik, *Phys. Stat. Sol. B* **128,** 591 (1985).
11. M. C. Aronson, J. L. Sarrao, Z. Fisk, M. Whitton, and B. L. Brandt, *Phys. Rev. B* **59,** 4720 (1999).
12. J. M. Tarascon, J. Etourneau, J. M. Dance, P. Hagenmuller, R. Georges, S. Angelov, and S. v. Molnar, *J. Less-Common Met.* **82,** 277 (1981).
13. K. A. Schwetz, Personal Communication, 1999.
14. K. A. Schwetz, M. Hoerle, and J. Bauer, *Ceram. Internatl.* **5,** 105 (1979).
15. R. A. Smith, "Wave Mechanics of Crystalline Solids." Chapman & Hall, London 1961.
16. G. Lucovsky, *Solid State Commun.* **3,** 299 (1965).
17. A. Hasegawa and A. Yanase, *J. Phys. Coll. C* **5** (Suppl. 6), 41, 377 (1980).
18. R. Schmechel and H. Werheit, *J. Phys.: Condens. Matter* **11,** 6803 (1999).
19. R. Schmechel and H. Werheit, *J. Solid State Chem.* **154,** 61 (2000).